Article

Not peer-reviewed version

Chronic Low Dose Rate Radiation-Induced Persistent DNA Damage and miRNAs/mRNAs Expression Changes in the Mouse Hippocampus

Hong Wang , Salihah Lau , Amanda Tan , FENG RU Tang *

Posted Date: 29 August 2024

doi: 10.20944/preprints202408.2168.v1

Keywords: low dose rate; chronic irradiation; neonatal; Brain; blood; cellular; miRNA and mRNA

Article

Chronic Low Dose Rate Radiation-Induced Persistent DNA Damage and miRNAs/mRNAs Expression Changes in the Mouse Hippocampus

Hong Wang, Salihah Lau, Amanda Tan and Feng Ru Tang *

Radiation Physiology Lab, Singapore Nuclear Research and Safety Initiative, National University of Singapore, Singapore

* Correspondence: tangfr@gmail.com

Abstract: Our previous study demonstrated that the acute high-dose rate (3.3 Gy/minute) gamma irradiation of postnatal day 3 (P3) mice with 5Gy induced depression and drastic neuropathological changes in the dentate gyrus of the hippocampus of the adult mice. The present study investigated the effects of chronic low-dose-rate (1.2mGy/h) gamma irradiation from P30 to P180 with a cumulative dose of 5Gy on animal behaviour, hippocampal cellular change, miRNA and mRNA expression in the hippocampus and blood in female mice. The radiation exposure did not significantly affect the animal's body weight and neuropsychiatric changes such as anxiety and depression examined by neurobehavioural tests including open field, light-dark box, elevated plus maze, tail suspension test and forced swim test. Immunohistochemical staining did not detect any obvious loss of mature and immature neurons (NeuN and DCX) or any inflammatory glial response (IBA1, GFAP, and PDGFR1). Nevertheless, r-H2AX foci in the stratum granulosum of the dentate gyrus were significantly increased, suggesting the chronic low dose rate irradiation induced persistent DNA damage foci in mice. miRNA sequencing and qRT-PCR indicated an increased expression of miR-448-3p and miR-361-5p, but decreased expression of miR-193a-3p in the mouse hippocampus. Meanwhile, mRNA sequencing and qRT-PCR showed a reduced expression of Ccn1, Fli1, Fosb, Ets1, Hs3st5, and Eif4ebp1, but enhanced expression of Cort, Foxh1, and Opalin. Database searching by miRDB and TargetScan predicted that FLI1 and HS3ST5 are the targets of miR-448-3p, and Eif4ebp2 is the target of miR-361-5p. miRNA/mRNA sequencing and qRT-PCR results in blood showed the increased expression of miR-6967-3p and the decreased expression of its target S1pr5. The interactions of these miRNAs and mRNAs may contribute to the chronic low dose rate radiation-induced persistent DNA damage.

Keywords: low dose rate; chronic irradiation; neonatal; Brain; blood; cellular; miRNA and mRNA

Introduction

It is widely accepted today that high dose/dose rate gamma irradiation induces harmful effects on the central nervous system (CNS), especially on the developing brain which is particularly vulnerable to deleterious effects. Irradiation exposure during the prenatal period may have a broad spectrum of consequences, including congenital abnormalities, mental retardations, developmental delays, behavioural alterations, and functional deficits, varying on the different doses [1–3]. The germ cells in the testes and ovaries of mice have almost obliterated on gestation day 18 foetuses irradiated with continuous medium-dose-rate (200 or 400 mGy/day) gamma-rays throughout the entire gestation period [4]. Very recently, we found that in prenatally irradiated B6C3F1 mice (100 mGy/d for 18 days), there were no cellular changes including newly generated immature neurons in the subgranular zone, mature neurons and glial cells in the hilus of the dentate gyrus [5]. Substantial negative effects on the developing human brain have been observed among children exposed to radiation during the gestational period at the atomic explosions of Hiroshima and Nagasaki [6,7] as

 doi:10.20944/preprints202408.2168.v1

well as over the time of the Chernobyl and Fukushima accidents [1,8,9]. Long-term cytogenetic effects indicated by the prevalence of chromosome aberrations were observed in children prenatally exposed to the Chernobyl nuclear accident [10]. The effects of prenatal irradiation on the development of cerebral electrical activity were investigated in human beings as early as 1968 [11]. Nevertheless, the consequences of post-natal irradiation exposure have not been extensively studied, especially after the low-dose-rate chronic gamma radiation exposure.

The development of the hippocampus plays an important role in its physical maturation. High-dose rate (3.3 Gy/m) acute gamma irradiation (5Gy) of day 3 mice has induced depression behaviour in adults accompanied by the hypoplasia of the infrapyramidal blade of the stratum granulosum as well as the impaired neurogenesis and cell division in the dentate gyrus [12]. A very recent study indicated that a fractionated gamma radiation in neonatal C57BL/6 at cumulative doses (0.1, 1, and 5 Gy) caused mouse behaviour changes dose-dependently: the low-dose gamma irradiation resulted in an increase in anxiety, while the raised dose caused a decrease in anxiety behaviour compared to control animals [13]. Moreover, Tanaka et al. reported that mice chronically exposed to low-dose-rate gamma rays from 8 weeks of age had significantly shorter life spans than non-irradiated mice [14] due to early death from a variety of neoplasms [15]. This evidence indicated that neonatal or adult gamma radiation in mice causes behavioural or cellular changes. Acute X-ray irradiation with 2 Gy at postnatal day 3 induced the impairment of spatial learning and memory and anxiety in adult mice, accompanied by the increased levels of γH2A histone family member X (γ-H2AX) [16]. An extensive induction of γH2AX foci was observed in different brain regions at 1 day after 5Gy gamma irradiation at postnatal days 3, 10, and 21 in mice, and lasted for 15 months after irradiation [17], suggesting that γ-H2AX serves as a marker for gamma radiation-induced DNA damage and be related to the animal behaviour changes.

In the previous experimental designs from different research groups, with no fixed total dose, dose rate or duration, it is difficult to determine whether the radiation-induced changes are related to the total dose, dose rate or duration. Given that our previous study with acute high-dose rate irradiation of postnatal day 3 mice with 5Gy induced obvious pathophysiological changes (Wang et al., 2021), in this study, we aimed to examine the effects of chronic low-dose-rate gamma irradiation for half a year with a cumulative dose of 5Gy on animal neuropsychiatric changes. Relevant hippocampal cellular miRNA and mRNA changes were also investigated. Meanwhile, blood miRNA and mRNA changes were also detected in order to correlate these changes to those in the hippocampus, and explore the possibility of using blood miRNAs and mRNAs as biomarkers to predict low-dose rate irradiation--induced brain pathophysiological changes.

Materials and Methods

1.1. Animals and Irradiation

Postnatal day 1 Balb/c pups with dams were purchased from InVivos Pte. Ltd. (Singapore), and housed in the Department of Comparative Medicine Facility, National University of Singapore. From postnatal day 3 (P3) onwards, pups with dams were continuously exposed to whole-body ^{137}Cs gamma rays (23.5h/daily exposure, 0.5h for animal feeding and cage cleaning) with a dose rate of 1.2mGy/h (G10-1-12 Gamma Beam Irradiator, GA, USA). By postnatal day 21, pups were weaned, and male and female pups were separated and continuously exposed to radiation with a low dose rate of 1.2mGy/h up to 180 days (a total accumulated dose of ~5Gy). Mice were then moved to a normal mouse room with background radiation. The radiation dose rate was monitored during irradiation with MAX 4000 Plus electrometer (Standard Image, WI, USA). The accumulated dose was measured with Nanodots (LANDAUER IL, USA) which were placed in each cage. The animal experimental protocols were approved by the Institutional Animal Care and Use Committee (IACUC), National University of Singapore (IACUC number: R20-0220). A total of 24 female mice (control: n=9; irradiated group: n=15) including age-matched non-irradiated controls was used in the study. All the animals had ad libitum feed and water supply. They were maintained under the following conditions: a 12h light/12 h dark cycle and constant temperature of 22 ℃, weekly cage change, and daily health monitoring. Animal body weight was measured weekly for the first 1

 doi:10.20944/preprints202408.2168.v1

month, biweekly for the second and third months, then continuously monitored, and weighed before mice were euthanized. Efforts were made to minimize the number of animals used throughout the study.

2.2. Behavioural Studies

Fourteen months after irradiation, irradiated and age-matched control Balb/c female mice were tested in open field (locomotor), light-dark box, elevated plus maze, tail suspension and forced swim tests.

2.2.1. Open Field (Locomotor) Test

The open field was done in an empty and opaque box with the dimensions 50 cm x 50 cm. The arena is divided into center and peripheral areas in the software to track the distance travelled and time spent in each area. The mouse was placed in the center area at the start of the test and was allowed to explore for 30 minutes to observe behavior. The ANY-maze software (ANY-maze, Wood Dale, IL, US) detects the center of the mouse's body, thus only detecting entry and tracking time and distance once half of the mouse's body is in the area.

2.2.2. Light Dark Box

Mice were placed in the light box, and the time spent in the light and dark box as well as distance travelled in the light box were recorded by ANY-maze (ANY-maze, Wood Dale, IL, US). The sizes of light and dark boxes are the same 50cm X 25cm.

2.2.3. Elevated Plus Maze

The maze was elevated to 50 cm in height. The size of the open and closed arms was 5cm X 30 cm and the centre was 5cm X 5cm. Animals were placed in one closed arm and recorded for 10 minutes. The time spent and distance travelled in the open and closed arms and the centre were calculated by ANY-maze (ANY-maze, Wood Dale, IL, US).

2.2.4. Tail Suspension Test

Mice were suspended by their tails that were taped to a hook for 6 min. Immobility time in terms of no limb movements for 3 seconds or more, was detected by the ANY-maze (ANY-maze, Wood Dale, IL, US). Immobilization is regarded as an indication of depression-like behaviour.

2.2.5. Forced Swim Test

A cylinder of 20cm diameter was filled with water (temperature: 24-26^{0}C). The mice were put inside and freely swam for 8 minutes. The animal movement was recorded and analysed using ANY-maze (ANY-maze, Wood Dale, IL, US). Immobilization time (the animal remained almost immobile without limb movements for 3 seconds or more) was used as a parameter to indicate depression-like behaviour.

2.3. Sample Collection

All female mice were sacrificed at 64 weeks of age by carbon monoxide asphyxiation after which blood samples were collected via cardiac puncture and then subjected to necropsy (gross examination).

0.5 mL whole blood was transferred to 2 mL tubes pre-loaded with 1.3ml RNAlater solution and stored frozen at -80°C until analysed. The whole brain was dissected and separated sagittally into the left and right hemispheres. The right hemisphere was fixed in 4% paraformaldehyde for 24h, then transferred to 30% sucrose in 0.1M phosphate buffer (pH: 7.4) for immunohistochemistry. The left hippocampus was dissected from the left hemisphere, and stored in -80^{o}C for RNA extraction.

 doi:10.20944/preprints202408.2168.v1

2.4. Immunohistochemical Staining

Sagittal sections of the right hemisphere were cut at 40 μm thickness. A series of alternative 6 sections were collected in 24 well plate with PBS. After being treated with 3% H_2O_2 and blocked with serum, free-floating sections were incubated with antibodies overnight. Six antibodies were used in immunostaining, namely newly generated neuronal marker doublecortin (DCX, 1: 500, Santa Cruz Biotechnology Inc., CA, USA), mature neuronal marker NeuN (1: 1000, Invitrogen, MA, USA), oligodendrocyte precursor cell marker platelet-derived growth factor receptor alpha 1 (PDGFR1, 1: 200, Cell Signaling Technology, MA, USA), astrocyte marker glial fibrillary acidic protein (GFAP, 1: 200, Cell Signaling Technology, MA, USA), microglial marker ionized calcium-binding adapter molecule 1 (IBA1, 1: 200, Cell Signaling Technology, MA, USA), and DNA damage and repair marker gamma H2A histone family member X (γH2AX,1: 200, Cell Signaling Technology, MA, USA). The sections were washed for two times with PBS-triton x-100, and then incubated with respective secondary antibodies. Avidin–biotin complex (ABC) reagent (Vector Laboratories Inc., Burlingame, CA, USA) was added and incubated for 30 minutes. After reaction in DAB Peroxidase Substrate (Vector Laboratories Inc., Burlingame, CA, USA), the sections were then washed, mounted on slides, counterstained and covered with cover slips.

Seven to nine immunostained sections were photographed under microscopy (Leica Microsystems GmbH, Wetzlar, Germany). The Stereologer System (Stereology Resource Center, Biosciences Inc. Tampa, FL, USA) was employed to analyse the number of NeuN, PDGFR1, and GFAP immunopositive cells in the hilus; IBA1 immunopositive cells in the hilus and stratum granulosum, indicated as the number/volume (mm^3). γH2AX foci in the stratum granulosum were counted and indicated as the number/area (mm^2). DCX immunopositive cells in the subgranular zone were counted and indicated as a number/per subgranular length (mm).

2.5. RNA Extraction from the Hippocampus and Whole Blood

RNA extraction from the left hippocampus was performed in 3 non-irradiated control and 3 irradiated mice using the miRNeasy Mini Kit (Qiagen, Hilden, Germany) according to the manufacturer's instructions. The hippocampus was homogenized in 700μl QIAzol lysis reagent, placed at room temperature for 5 min, added with 140 μl chloroform, and shaken vigorously for 15s. The tube was centrifuged for 15 min at 12000 x g at 4°C. After centrifugation, the samples separate into 3 phases. The upper colourless aqueous phase containing RNA was collected into a new tube and mixed with 1.5 volumes of 100% ethanol. The above mixture was loaded into a RNeasy Mini spin column and centrifuged at ≥8000 x g for 15s. The column was washed and centrifuged. RNA from the column membrane was finally eluded with 40 μl RNase-free water.

RNA from whole blood was isolated using Mouse RiboPure™-Blood RNA Isolation Kit (Life Technologies Holdings Pte Ltd. Singapore). After centrifugation of blood in pre-loaded RNAlater solution, the supernatant was removed. The cell pellet was reconstituted by adding a lysis solution (3M sodium acetate, and acid phonol:chloroform), centrifuged, and the aqueous upper phase was recovered and mixed with 100% ethanol. The sample was then vacuum-filtered through a Filter Cartridge, washed, and eluted with nuclease-free water. RNA concentration was measured using the Nanodrop and Bioanalyzer system (Agilent Technologies, Santa Clara, CA, USA).

2.5. Systematic miRNA Sequencing (miRSeq) and mRNA Sequencing Analysis

miRSeq and mRNA sequencing of the hippocampus and blood was carried out using the DNB SEQ platform (BGI, Beijing, P.R. China). Based upon p Value less than 0.05 and fold change more than 1.5 between control and irradiated samples analysed by DESeq2 method, 140 and 186 differentially expressed miRNAs in the hippocampus and blood were detected respectively. Similarly, 107 and 462 differentially expressed mRNAs were detected in the hippocampus and blood respectively.

2.5. Real-Time Quantitative Reverse Transcription PCR (qRT-PCR) Analysis of miRNA

 doi:10.20944/preprints202408.2168.v1

miScript II RT kit (Qiagen, Hilden, Germany) was used to reversely transcribe RNA into cDNA. 20 μl reaction mixture contained 5 μL template RNA, 2 μL reverse transcripts mix, 4 μL 5x HiSpec buffer, 2 μL 10x nucleotide mix, and 7 μL nuclease-free water. The mixture was incubated at 37 °C for 1 h followed by 95 °C for 5 min.

For real-time PCR, 20 μL of reaction mixture was prepared as: 10 μL 2x miScript SYBR green PCR master mix, 4 μL nuclease-free water, 2 μL diluted cDNA, 2 μL 10x miScript universal primer and 2 μL primer for target miRNAs (Table 1). PCR reactions were denatured at 95 °C for 15 min, followed by 40 cycles of denaturation at 94 °C for 15 sec, annealing at 55 °C for 30 sec, and extension at 70 °C for 30 sec. QuantStudio 6 Real-Time PCR Systems (Thermo Fisher Scientific, Waltham, MA, USA) was used to carry out PCR amplification and fluorescence data collection. The expression of miR-68 was used as an internal control.

Table 1. miRNA sequences for qRT-PCR in hippocampus and blood.

miRNA	Primer sequence
mmu-miR-448-3p	TTGCATATGTAGGATGTCCCAT
mmu-miR-193a-3p	AACTGGCCTACAAAGTCCCAGT
mmu-miR-361-5p	TTATCAGAATCTCCAGGGGTAC
mmu-miR-450-5p	CGTTTTGCGATGTGTTCCTAAT
mmu-miR-20a-3p	ACTGCATTACGAGCACTTAAAG
mmu-miR-495-3p	AAACAAACATGGTGCACTTCTT
mmu-miR-199b-3p	ACAGTAGTCTGCACATTGGTTA
mmu-miR-101a-5p	TCAGTTATCACAGTGCTGATGC
mmu-miR-10b-5p	TACCCTGTAGAACCGAATTTGTG
mmu-miR-1298-3p	CATCTGGGCAACTGATTGAACT
mmu-miR-124b-3p	TCAAGGTCCGCTGTGAACACGG
mmu-miR-16-2-3p	GACCAATATTATTGTGCTGCTTT
mmu-miR-7037-5p	AAGGTGGCCACAGGAGATCATGGT
mmu-miR-206-3p	TGGAATGTAAGGAAGTGTGTGG
mmu-miR-1947-5p	AGGACGAGCTAGCTGAGTGCTG
mmu-miR-199b-3p	ACAGTAGTCTGCACATTGGTTA
mmu-miR-5134-3p	ACGGGTGGCCCTCTTTCTGCAG
mmu-miR-296-5p	AGGGCCCCCCCTCAATCCTGT
mmu-miR-7024-5p	TTGGGGGATGGGTTGCTTGGC
mmu-miR-6967-3p	TCATCTTTATCTCTCCCCAG
mmu-miR-68	GCTGTACTGACTTGATGAAAGTAC

2.5. Real Time RT-PCR Analysis for mRNA

RNA was reverse transcribed into cDNA using Maxima first strand cDNA synthesis kits (Thermo Fisher Scientific, Waltham, MA, USA). 20 μL reaction included: 2 μL Maxima Enzyme Mix, 4 μL 5X Reaction Mix, 1 μg RNA, and nuclease-free water. The mixture was thereafter incubated at 25 ˚C for 10 min, 50 ˚C for 45 min, and 85 ˚C for 5 min.

A master mix of 20 μL for real-time PCR was prepared as follows: 10 μL 2x Maxima SYBR Green qPCR Master Mix, 2 μL diluted cDNA, 2 μL 10x forward and reverse primers for target genes (Table 2), and 4 μL nuclease-free water. QuantStudio 6 Real-Time PCR Systems (Thermo Fisher Scientific, Waltham, MA, USA) was used to carry out PCR amplification. The mixture was initially denatured at 95 ˚C for 10 min, then 40 cycles of: denaturation at 95 ˚C for 15 sec, annealing at 60 ˚C for 30 sec, extension at 72 ˚C for 30 sec. The fluorescence data was collected after the extension step. The expression of GAPDH was used as internal control.

Table 2. Primer sequences for mRNA qRT-PCR in hippocampus and blood.

 doi:10.20944/preprints202408.2168.v1

Gene name	Primer sequence
Ccn1 F	CGTCCTTGTGGACAACCAGT
Ccn1 R	CATGATGCTTGCGCTTCTCC
Cort F	TGTGAGATGCCAACGAGACC
Cort R	TGTTGTCGGTAGCGAGCATT
Foxh1 F	CAGGCTGAAACTGGCTCAGA
Foxh1 R	AGGAGCTAGAGGGTCCAGTG
Fli1 F	ATCTGAAGGGGCTACGAGGT
Fli1 R	TGACTCTCCGTTCGTTGGTG
Opalin	GATGAGCCCCGTATGTCCTG
Opalin	GCCTGTCCTAACTTGTGCCA
Fosb F	CCTTCAGTCCCAAAGACGAGT
Fosb R	GGGTGGGGTTTGGGATTAGG
Ets1	CGGTCAGCGGGAATTTGAGA
Ets1	ATCTCCTGGCCACCTCATCT
Hs3st5	GGCGTGTCTGAATGTAGGCT
Hs3st5	CTCCTTCCCCTCTAGCACCT
Eif4ebp2 F	AGCAGAAGTGCCAACACCTT
Eif4ebp2 R	GATGTGGAAAATGGCCCGGT
Zfhx4 F	TAAGGCTGAGACTTGGCTGC
Zfhx4 R	CCCTGTCAGGCTCTATCCCT
YOD1 F	TTTGACCCCATTTCCCCAGT
YOD1 R	TAGGTTGGCCAGTAACCCCT
Hivep3 F	CCCACCATCCCCACTGAAAG
Hivep3 R	GGCAACCCGGGCTCCTTTAT
Chrm5 F	GCTTGTCAAGGTGCAAGGTC
Chrm5 R	GTCCCTGCTGTTCTTCACAGA
Cox6b2 F	TTTTCTCCCGTGCTCTTGGG
Cox6b2 R	AGTACTCGCAGGGTTGTGTG
TSPO F	CTTGGGTCTCTACACTGGTC
TSPO R	AGACTTTATTTAGCTTTAAAACACC
Notch3 F	CTCTCCCTGCCTCAACTTCC
Notch3 R	CTCCCAAATGTCCCCTGACC
Kifc1 F	GAGCCTGCAAAGAAACGGAC
Kifc1 R	TATATGCCACCTACTGCCAGG
Orc1 F	AAGTGTTGGAGAAGTTACGGT
Orc1 R	GACCAACCCACCAGGGATTT
Apoc1 F	GGGCGGTGGTGAATACTAGC
Apoc1 R	TGGCTACGACCACAATCAGG
Rnf43 F	AATTTGTTTCATCCCCGTGCC
Rnf43 R	CTCCCATCGTCACTGCGAAT
Ahnak F	CAGTCAGCACTGCGACCTC
Ahnak R	TTTGCAGGACTCTGCTCAGG
Tppp3 F	TAGAAGCCGGGTGGCATGG
Tppp3 R	GTTCTTTGTGGGAGCCCGTA
Cdkn2c F	CCGGCACAGTACCTTCAGAG
Cdkn2c R	AGCTCAGGCTCTTCACTGCAA
S1pr5 F	ACACCAAATGCCCAGCTTAC
S1pr5 R	AAGTCTCCTGTAACCGGCAC
Mcpt4 F	AGAATCTCTCTCCAAGCTGT

 doi:10.20944/preprints202408.2168.v1

Mcpt4 R	GTAAGGGCGAGAATGTGGTC
Rbpms F	ATTGCCTCAAGAGGAGCAGG
Rbpms R	GGGCGGTCTATCTGACATGG
Vcam1 F	ACTTTCTAATTCATGGTAGAATGGC
Vcam1 R	CAATGAAGAAACAGGTCCCCG
Lepr F	TGATAATGGTGTGACGGTTGC
Lepr R	GGAAGCTTTCACACACTGAA
Slc15a2 F	CAGGGAACGAGCTTGGGAAT
Slc15a2 R	GCAGTTGTCTGGGGAAAGGA
Mlxipl F	CCTGAGCATCTGCAGCCTC
Mlxipl R	ATGACAGCCTCAGGTTTCCG
GAPDH F	ACCACAGTCCATGCCATCAC
GAPDH R	TCCACCACCCTGTTGCTGTA

2.5. Statistical Analyses

The Student's t-test was used to compare the body weight, behavioural changes, immunohistochemical staining, and qRT-PCR between the non-irradiated control and irradiated mice. $p<0.05$ was considered statistically significant. miRNAs and mRNAs analyses were based on the parameters $|log2FC| > 0.585$ and $P<0.05$, which was considered as significantly differential expression of DEseq2.

Results

3.1. Body Weight and Behavioural Changes

Animal body weight increased one week after gamma irradiation and then did not show any significant difference between the control and irradiated groups from two weeks until 64 weeks (Figure 1).

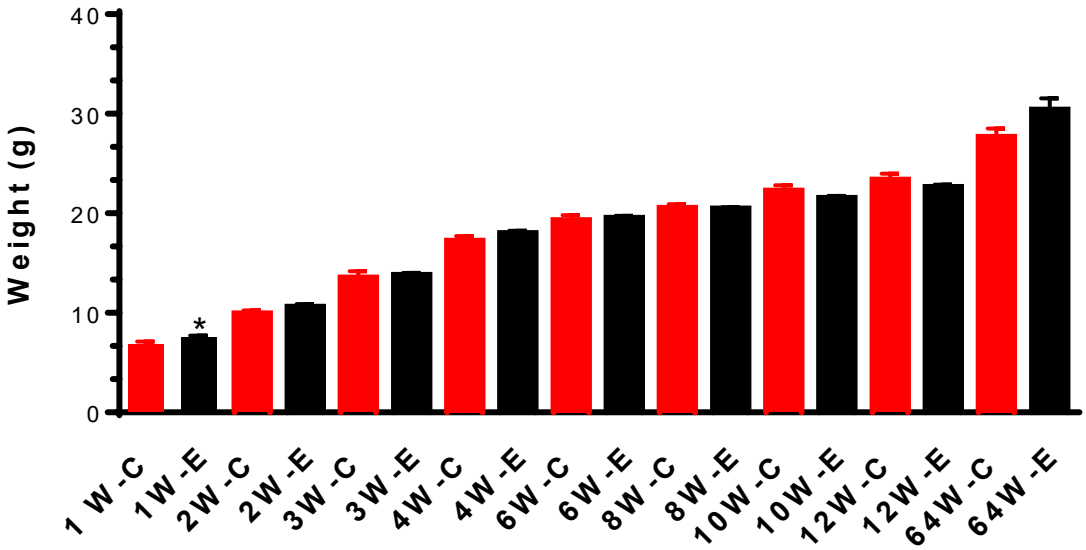

Figure 1. Weight measurement indicates that chronic irradiation with a dose rate of 1.2mGy/h does not affect weight gain from 2 weeks during irradiation until 64 weeks after the first irradiation started. Animal weight gain was increased significantly during the first week of irradiation. * $p < 0.05$.

 doi:10.20944/preprints202408.2168.v1

The open field test showed that the control and the irradiated animals spent almost the same time in the center and peripheral areas (Figure 2A). The distance travelled also showed no differences in these two areas (Figure 2B). In the light-dark box test, the time spent and distance travelled in the light box did not differ between control and experimental groups (Figure 2C & D). Moreover, animals did not exhibit any changes in anxiety-like behaviour in the elevated plus maze indicated by the time spent and distance travelled in the center and open and closed arms (Fig. E & F). Tail suspension and forced swim tests did not show a significant difference in immobile time between the control and the irradiated mice either (Figure 2G). All the tests demonstrated that chronic low-dose-rate post-natal gamma irradiation did not induce anxiety-like behaviour, stress and depression changes in mice.

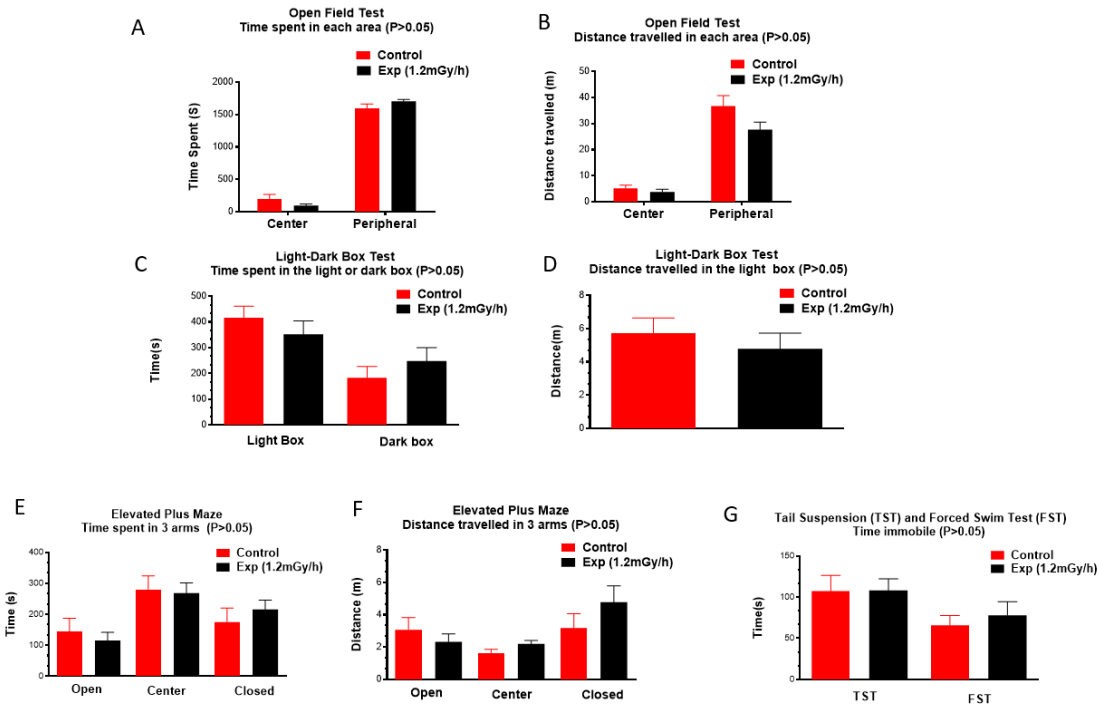

Figure 2. Neurobehavioural tests do not show chronic irradiation-induced anxiety and depression: Time spent (A) and distance travelled (B) in open field test; Time spent (C) and distance travelled (D) in the light-dark box; Time spent (E) and distance travelled (F) in three areas in the elevated plus maze. Time immobile in tail suspension test and forced swim test (G).

3.2. Immunohistochemistry Examination

Immunohistochemical study did not show a significant difference in the number of mature neurons (NeuN) in the hilus (Figure 3A, A1, G, microglia (IBA1) in the hilus and the stratum granulosum (Figure 3B, B1, G), astrocytes (GFAP) (Figure 3C, C1, G) and oligodendrocyte precursor cells (PDGFR1) (Figure 3D, D1, G) in the hilus of the dentate gyrus of the hippocampus between the control and irradiated groups. There was also no change of the number of immature neurons (DCX) in the subgranular zone of the dentate gyrus (Figure 3E, E1, H). However, r-H2AX immunostaining showed a greatly significant increase in the irradiated mice compared with the control group (Figure 3F, F1, I), indicating persistent DNA damage foci even 64 weeks after post-natal irradiation.

 doi:10.20944/preprints202408.2168.v1

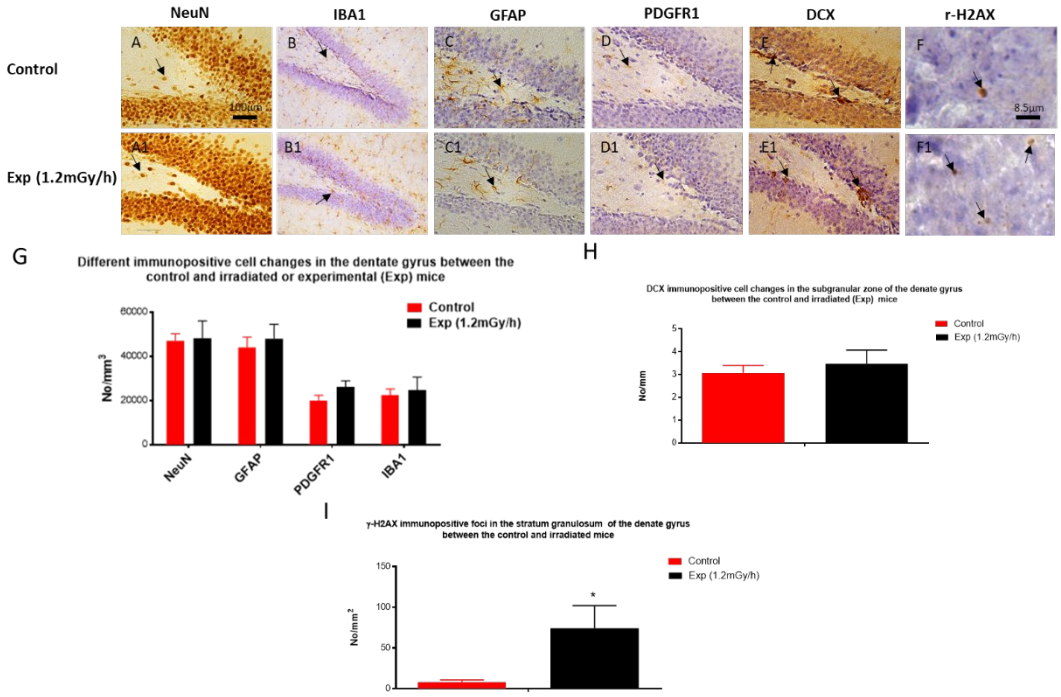

Figure 3. Immunohistochemical staining in hippocampus of control and experiment mice. A&A1: NeuN immunopositive mature neurons (arrow) in the hilus; B&B1: IBA1 immunopositive microglia (arrow) in the hilus and the granule cell layer: C&C1: GFAP immunopositive astrocytes (arrow); D&D1: PDGFRα immunopositive oligodendrocyte precursor cells (arrow); E&E1: DCX immunopositive immature neurons (arrow) in the subgranular zone; F&F1: γ -H2AX immunostaining shows DNA damage foci in the granule cells. Scale bar =100μm in A applies to B-E, A1-E1; Scale bar =8.5μm in F applies to F1. G&H&I: statistical results. * $p < 0.05$.

3.3. mRNA Sequencing and qRT-PCR in the Hippocampus

Sequencing analysis indicated 107 differentially expressed mRNAs in the hippocampus of irradiated mice ($p<0.05$ and fold change > 1.5 (Suppl 1)). 41 mRNA were upregulated, while 66 were down-regulated. Among them, we selected 20 genes (Figure 4A) which were related to DNA damage or neurological disorders, to validate by qRT-PCR (Figure 4A, B, C). The results showed that the expression of cellular communication network factor 1 (Ccn1), friend leukemia integration 1 transcription factor (Fli1), protein fosB (Fosb), E26 transformation–specific sequence-1 (Ets-1), heparan sulfate-glucosamine 3-sulfotransferase 5 (Hs3st5), and Eukaryotic Translation Initiation Factor 4E Binding Protein 2 (eif4ebp2) was significantly down-regulated in the experimental group. In contrast, corticosterone (Cort), forkhead box protein H1 (Foxh1), and oligodendrocytic paranodal loop protein (Opalin) were up-regulated after gamma irradiation when compared with control mice (Figure 4B). The expression trend of these genes from qRT-PCR (Figure 4B, C) is consistent with the mRNA sequencing data indicated by heatmap (Figure 4A).

 doi:10.20944/preprints202408.2168.v1

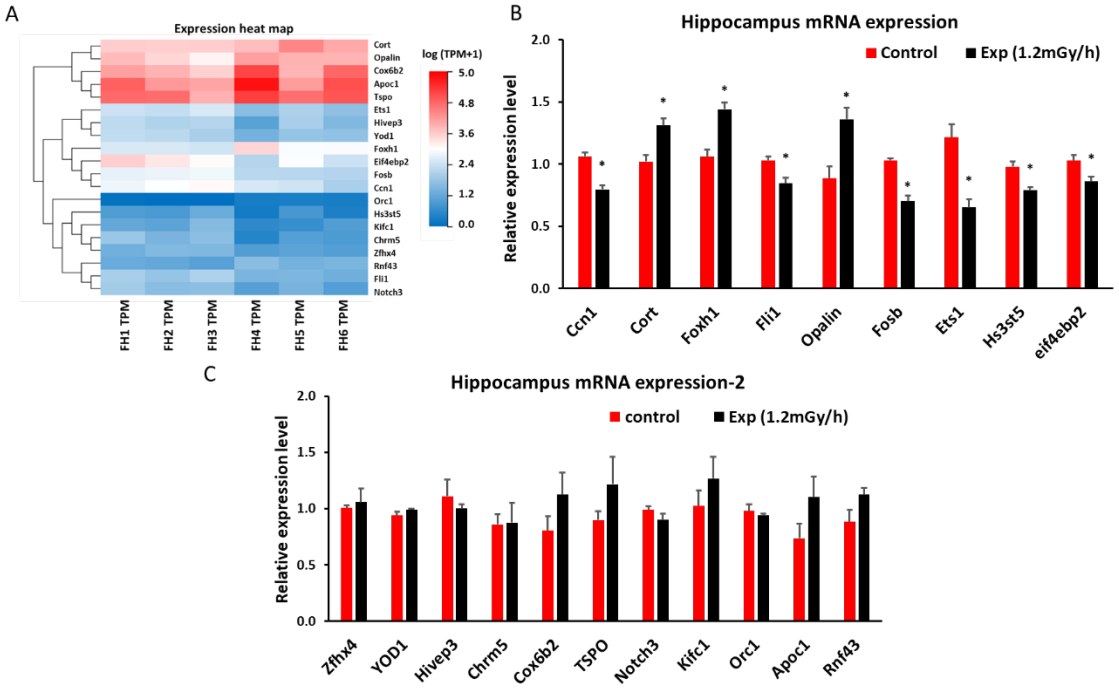

Figure 4. Low dose rate irradiation-induced hippocampal mRNA changes: (A) Heatmap of mRNA changes from mRNA sequencing in the control and experiment mice. (B &C) qRT-PCR indicates a significant down-regulation of Ccn1, Fli1, Fosb, Ets1, Hs3st5 and eif4ebp2 genes, and up-regulation of Cort, Foxh1, and Opalin genes (B, * $p < 0.05$), but no significant changes of Zfhx4, YOD1, Hivep3, Chrm5, Cox6b2, TSPO, Notch3, Kifc1, Orc1, Apoc1, and Rnf43 (C, $P>0.05$).

3.4. miRNA Sequencing and qRT-PCR in the Hippocampus

Sequencing analysis showed 140 differentially expressed miRNAsin the hippocampus of irradiated mice ($p<0.05$ and fold change > 1.5 (Suppl 2)). Based on database search on miRDB and TargetScan of interaction of these miRNA with the differentially expressed mRNA,10 miRNAs were chosen for validation by qRT-PCR (Figure 5A, B). The expression of two miRNAs, i.e., miR-448-3p and miR-193a-3p, decreased and was consistent with the miRNA sequencing results (Figure 5A&B). Both qRT-PCR and miRSeq indicated an increased expression of miR-361-5p. Targetscan indicated that that Fli1 and Hs3st5 might be the targets of miR-448-3p. Ets1 might be the target of miR-193a-3p.

 doi:10.20944/preprints202408.2168.v1

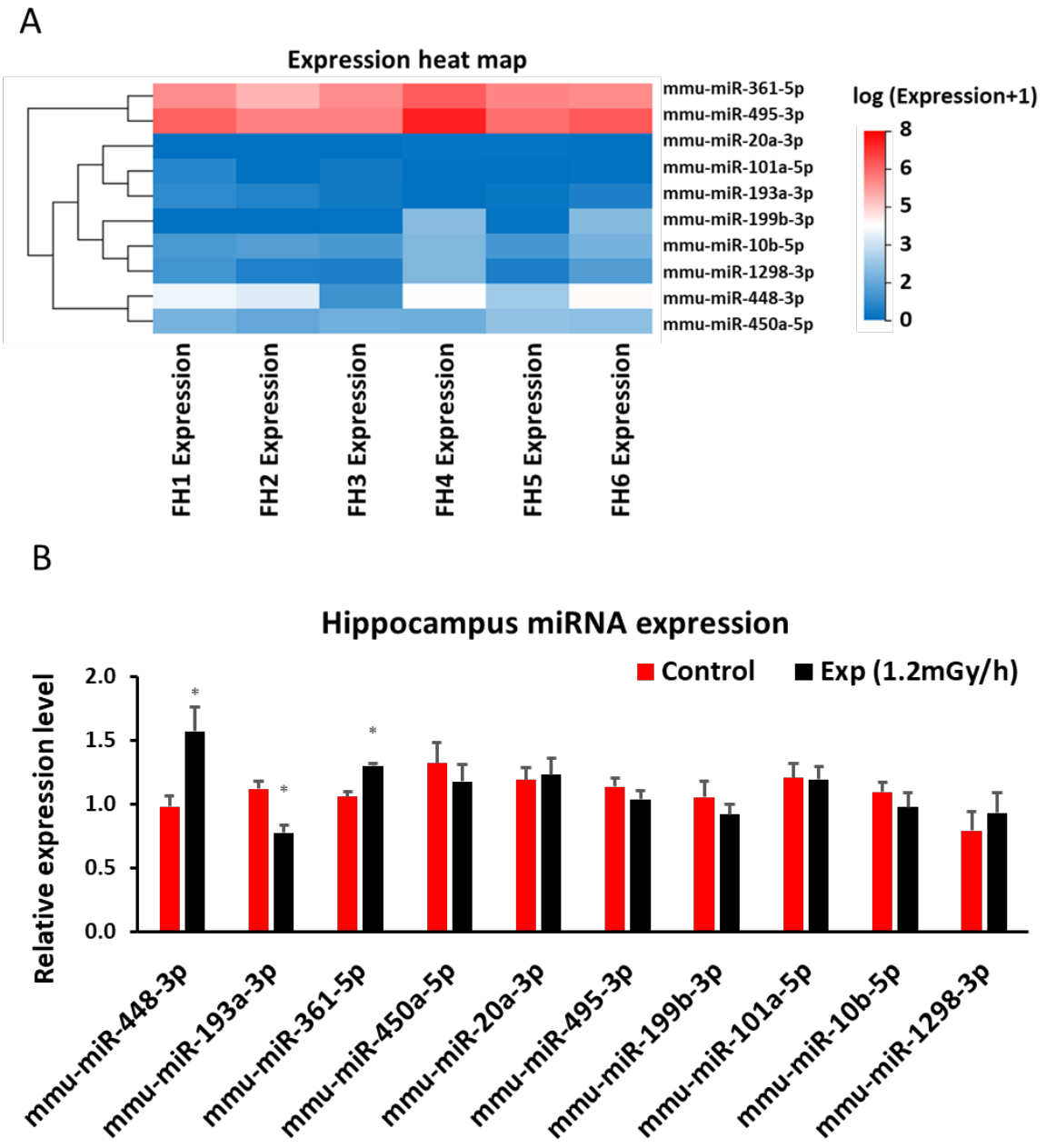

Figure 5. Low dose rate irradiation-induced hippocampal miRNA changes: (A) Heatmap of miRNA changes from miRNA sequencing in the control and experiment mice; (B) qRT-PCR indicates a significant down-regulation of miR-193a-3p and up-regulation of miR-448-3p and miR-361-5p in irradiated mice (* $p < 0.05$), but no changes for other miRNA investigated ($P > 0.05$).

2.5. miRNA Sequencing and qRT-PCR in Blood

Sequencing analysis indicated 186 differentially expressed miRNAs in the blood of irradiated mice ($p<0.05$ and fold change > 1.5 (Suppl 3)). When 10 miRNAs were selected for validation by qRT-PCR (Figure 6A&B), it was shown that miR-296-5p was down-regulated and miR-6967-3p was up-regulated in blood after gamma irradiation when compared with control group (Figure 6A&B).

 doi:10.20944/preprints202408.2168.v1

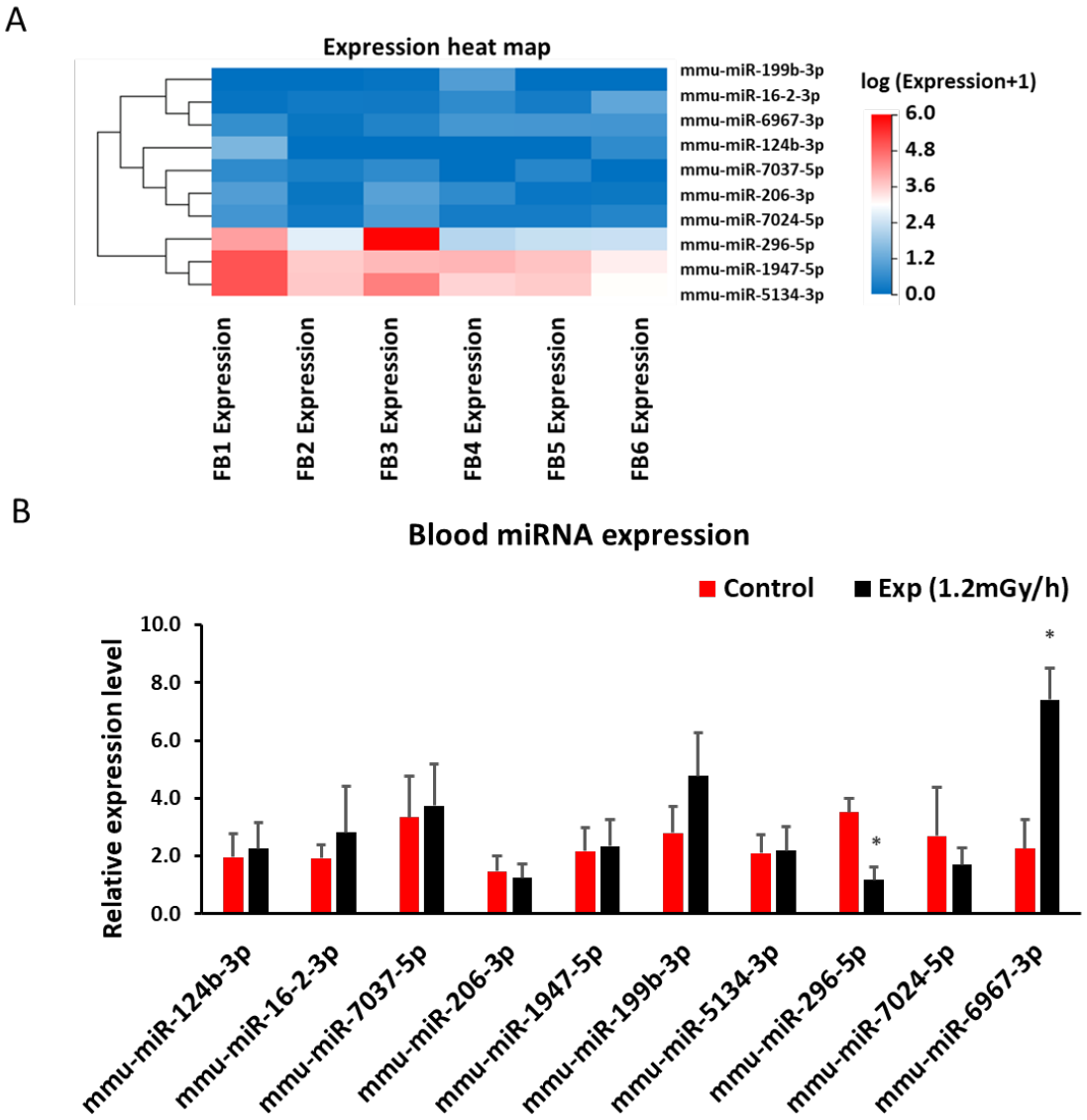

Figure 6. Low dose rate irradiation-induced blood miRNA changes: (A) Heatmap of miRNA sequencing results in the blood of control and experiment mice; (B) qRT-PCR indicates a significant down-regulation of miR-296-5p and up-regulation of miR-6967-3p (* $p < 0.05$), but no changes of other miRNAs in the blood of the control and irradiated mice.

2.5. mRNA Sequencing and qRT-PCR in Blood

Sequencing analysis showed 462 differentially expressed mRNAs in the blood of irradiated mice ($p<0.05$ and fold change > 1.5 (Suppl 4)). qRT-PCR study of 10 genes related to DNA damage or neurological disorders showed that the expression of Tubulin polymerization promoting protein family member 3 (TPPP3), sphingosine-1-phosphate receptor 5 (S1PR5), and RNA-binding protein with multiple splicing (RBPMS) was decreased, while the expression of Leptin receptor (LEPR) was increased in mouse blood after gamma irradiation (Figure 7A&B). Targetscan suggested the interaction of miR-6967-3p and S1PR5.

 doi:10.20944/preprints202408.2168.v1

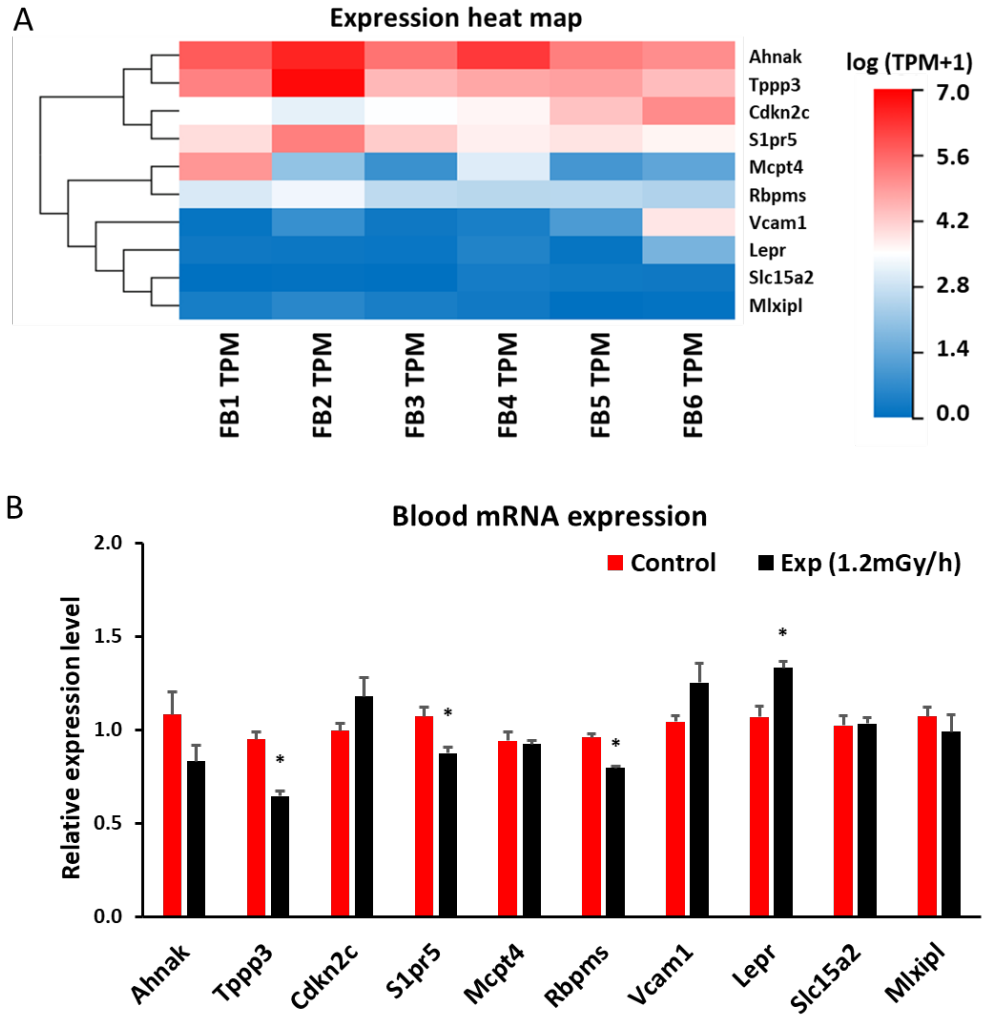

Figure 7. Low dose rate irradiation-induced blood mRNA changes: (A) Heatmap of mRNA sequencing results in the blood of control and experiment mice; (B) qRT-PCR indicates a significant down-regulation of Tppp3, S1pr5, Rbpms, and up-regulation of Lepr genes (* $p < 0.05$). but no changes of other mRNAs in the blood of the control and irradiated mice.

2.5. Venn Diagram Analysis of Differentially Expressed mRNA and miRNAs between Blood and Hippocampus

Venn diagram analysis indicated that 18 miRNAs and 2 mRNAs are differentially expressed in both hippocampus and blood respectively (Figure 8A, B, C). However, among 18 miRNAs, 11 miRNAs showed an opposite expression pattern, in terms of up- or down-regulation in blood, and down- or up-regulation in hippocampus. 5 down-regulated (miR-124b-3p, miR-1947-5p, miR-5134-3p, miR-7024-5p, and novel- miR143-3p) and 2 up-regulated miRNAs (miR-16-2-3p and miR-199b-3p) plus 2 down-regulated mRNAs (Ahnak and LOC118568304) were expressed in both hippocampus and blood (Figure 8C). The results indicated that blood markers after gamma irradiation may not reflect the changes in hippocampus.

 doi:10.20944/preprints202408.2168.v1

A

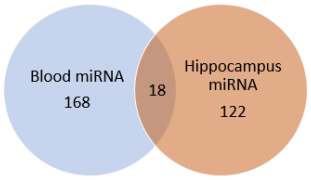

B

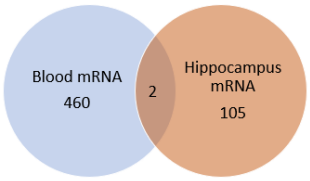

C

Gene Symbol	Type	Blood		Hippocampus	
		log2 (Exp/Con)	Pvalue(Exp/Con)	log2 (Exp/Con)	Pvalue(Exp/Con)
mmu-let-7i-3p	miRNA	1.179651326	1.80E-18	-0.610688369	3.28E-29
mmu-miR-124b-3p	miRNA	-2.038022547	0.002099885	-1.901103432	1.50E-10
mmu-miR-141-3p	miRNA	0.882542986	3.57E-05	-0.790181618	0.00895345
mmu-miR-16-2-3p	miRNA	2.186943818	0.001067967	2.22301788	0.024803991
mmu-miR-1947-5p	miRNA	-0.603681909	5.02E-11	-0.689410899	0.005580769
mmu-miR-199b-3p	miRNA	3.743337167	0.001037977	6.365975834	1.19E-39
mmu-miR-466i-5p	miRNA	-1.011550335	5.32E-05	0.668429028	0.012455565
mmu-miR-466p-5p	miRNA	3.743337167	0.020377255	-0.650514119	0.03308646
mmu-miR-5134-3p	miRNA	-1.038022547	2.18E-29	-1.268835216	0.006746193
mmu-miR-532-3p	miRNA	-0.781682793	0.00186336	0.849559484	4.41E-11
mmu-miR-669f-5p	miRNA	0.667569659	0.024385494	-0.621811748	0.009691699
mmu-miR-6952-3p	miRNA	-2.163553429	0.018294552	2.168570096	0.007898929
mmu-miR-7024-5p	miRNA	-1.230667625	0.032664096	-1.432333949	0.04227579
mmu-miR-96-5p	miRNA	2.006371573	0.009262883	-0.773953156	2.11E-20
novel-mmu-miR142-3p	miRNA	-1.993628427	0.009719027	0.790058473	0.03111244
novel-mmu-miR143-3p	miRNA	-1.38594585	1.18E-05	1.067739654	1.25E-05
novel-mmu-miR432-5p	miRNA	1.006371573	0.001374631	-0.687624851	1.11E-38
novel-mmu-miR489-3p	miRNA	-1.504590347	6.10E-05	-0.672284741	0.001211744
LOC118568304	mRNA	-0.728380102	0.033305663	-1.335442897	0.004196335
Ahnak	mRNA	-0.597190258	0.021621116	-0.726524812	6.81E-08

Figure 8. Low dose rate irradiation-induced differentially expressed miRNAs and mRNAs in both blood and hippocampus: A & B: Venn diagram of differentially expressed 18 miRNA (A) and 2 mRNA (B) in both blood and hippocampus of irradiated mice compared to the control; C. Table list of 18 miRNA and 2 mRNA differentially expressed in both blood and hippocampus.

Discussion

4.1. Main Findings

Based on our previous publication of acute high dose rate/dose (3.33Gy/m, 5Gy) irradiation induced-pathophysiological changes in the hippocampus [12], this study systemically investigated the effects of chronic low-dose-rate with cumulative high dose (dose rate: 1.2mGy/h, total dose: 5Gy) gamma irradiation from postnatal day 3 to day 180 on animal behaviour, hippocampal cellular change, miRNA and mRNA expression in the hippocampus and blood in female mice. It showed that the low dose rate gamma irradiation with a cumulative dose of 5Gy did not affect the animal body weight significantly except an increase for the first week. Neurobehavioural tests including open field, light-dark box, elevated plus maze, tail suspension test and forced swim tests, did not detect any significant neuropsychiatric changes such as anxiety and depression which had been found in our previous acutely irradiated mice [12]. NeuN and DCX immunohistochemical staining did not show obvious loss of mature and immature neurons in the dentate gyrus, which was very different from the acute irradiation at postnatal day 3 with 5Gy showing impairment of neurogenesis and hypoplasia of the low blade of granule layer [12,18]. IBA1, GFAP, and PDGFR1 immunostaining did not demonstrate any inflammatory glial response which has been observed after acute irradiation [19]. r-H2AX immunostaining indicated a significant increase of r-H2AX foci in the stratum granulosum of the dentate gyrus, suggesting chronic low dose rate irradiation-induced persistent DNA damage foci which have also been found after acute irradiation with the same dose [17]. miRNA sequencing and qRT-PCR indicated an increased expression of miR-448-3p and miR-361-5p, but decreased expression of miR-193a-3p in the mouse hippocampus. Meanwhile, mRNA sequencing and qRT-PCR showed a reduced expression of Ccn1, Fli1, Fosb, Ets1, Hs3st5, and Eif4ebp1, but enhanced expression of Cort, Foxh1, and Opalin. Database searching by miRDB and TargetScan predicted that FLI1 and HS3ST5 are the targets of miR-448-3p, and Eif4ebp2 is the target of miR-361-5p. miRNA/mRNA sequencing and qRT-PCR results in blood showed the increased expression of miR-6967-3p and the decreased expression of its target S1pr5. The interactions of these miRNAs and mRNAs may contribute to the chronic low dose rate radiation-induced persistent DNA damage.

4.2. Chronic Low Dose Rate Irradiation Did Not Induce Abnormal Cellular Changes in the Dentate Gyrus of the Hippocampus and Neuropsychiatric Abnormality

Post-natal high-dose rate acute gamma irradiation (5Gy) of postnatal day 3 mice induced depression behaviour in adults accompanied by impaired neurogenesis and cell division in the dentate gyrus (Wang, et al. 2021). Acute high-dose irradiation induces a complex network of cellular

 doi:10.20944/preprints202408.2168.v1

and molecular alterations, e.g., oxidative stress, systemic inflammation, DNA damage, and cell death. However, the research findings are controversial regarding the effects of low-dose or low-dose-rate gamma irradiation on behavioural, neurological or cellular changes. Male adult BALB/c mice showed no significant differences in the immobility times in the forced swim test after receiving 7 days of gamma irradiation at 0.6 mGy/h or 3.0 mGy/h (total doses 0.1 or 0.5 Gy) [20]. Female adult Sprague Dawley (SD) rats were continuously irradiated for 30 days (dose rates 6 and 20 mGy/h, with a total dose of 0.9 Gy and 3 Gy). This chronic low-dose γ-irradiation impaired the learning memory in rats, but none of the irradiated animals exhibited signs of anxiety or depression [21]. The image examination did not reveal any noticeable structural changes in the brain, but irradiation with 20 mGy/h caused neuronal damage in the rat hippocampus [21]. Very recently, we found that in prenatally irradiated B6C3F1 mice (100 mGy/d for 18 days), there were no cellular changes in immature neurons, mature neurons and glial cells, but a significant reduction in body weight, mass index (BMI) and exploratory behaviour in the open field test (Tang, et al. 2024). However, when pregnant Wistar rats were exposed to γ-irradiation from embryonic day E13 to E16 (0.7 mGy/min; total cumulative dose approximately 3 Gy), the adult offsprings showed a statistically significant decrease in numbers of hippocampal pyramidal and granule cells [22]. The diversity may be due to the differences in animal species, gender, age, behaviour test models, and examining methods. In this study, chronic post-natal low-dose-rate with cumulative high dose (dose rate: 1.2mGy/h, total dose: 5Gy) gamma irradiation did not induce the cellular, neurocognitive and psychiatric changes in female mice.

4.3. Chronic Low Dose Rate Irradiation Induced Persistent DNA Damage Foci

The phosphorylated histone r-H2AX has been demonstrated to form foci in nuclei and megabase chromatin domains after the DNA lesion on chromosomes. It has been well recognized as a biomarker for DNA damage from radiation exposure [23,24]. DNA double-strand breaks (DSBs) are the most relevant lesions in the ionizing radiation exposure-induced deleterious effects. DSBs are rapidly formed following the phosphorylation of H2AX histone at Ser-139. This procedure is believed to favour the recruitment or access of repair proteins [25]. In radiation research, r-H2AX has been used as a biodosimetry tool for radiation exposure assessment [24,26,27]. Very recently, Ramadhani et al. used an enzyme-linked immunosorbent assay (ELISA) to quantify γ-H2AX in male human peripheral blood mononuclear cells (PBMCs) after exposure to different doses of ^{60}Co, and showed that the ratio of γ-H2AX/total H2AX increased in a radiation-dose-dependent manner [24]. Chen et al. employed another method flow cytometry to measure γ-H2AX fluorescence in male BALB/c mouse blood exposed to X- ray, and observed that the fluorescence intensity values increased with radiation dose [27]. Mass spectrometry quantification of γ-H2AX was also developed as an estimation assay in human peripheral blood lymphocytes for low-level exposure to ionizing radiation [28]. Moreover, γ-H2AX induction was observed in a swine model [29], on patients after abdominal-pelvic and chest CT exams with very low-ionizing radiation exposure (doses of 15.67-63.45 mGy) [30], and in a rhesus macaque (Macaca mulatta) model after whole-body radiation exposure (^{60}Co) [31]. Our group also showed an extensive induction of γH2AX foci in different brain regions age-dependently at 1 day after 5Gy gamma irradiation at postnatal day 3, 10, and 21 [17]. These findings support our result that γ-H2AX immunopositive foci increased significantly in the mouse dentate gyrus after radiation exposure. Although this chronic low-dose-rate post-natal gamma irradiation did not significantly induce the morphological changes in the hippocampus, gamma irradiation-induced DNA damage could not be fully repaired and existed until 16 months. All the above evidence indicates that the increase of γ-H2AX levels is proportional to the irradiation doses and γ-H2AX may serve as a useful quantitative biomarker of radiation exposure at different doses. The quantitation of γ-H2AX foci may make a fast and accurate biological dosimeter for assessing the consequence of ionising radiation exposure in humans in the event of a radiological incident and evaluating the medical intervention in clinical use.

2.5. Chronic Low Dose Rate Irradiation Induced miRNA and mRNA Changes in the Hippocampus

 doi:10.20944/preprints202408.2168.v1

Our previous studies have demonstrated that miRNAs play an important role in brain morphological and behavioural changes induced by acute high-dose gamma irradiation in mice [12,19,32]. The γ-radiation activated miR-43a-5p/Tia1 pathway in the early life of mice was demonstrated to be related to the pathogenesis of adult depression [12]. The interaction of miR-181b-2-3p and its target SRY-related high-mobility group box transcription factor 21 (SOX21) plays a duel role in the brain inflammation and the impairment of neurogenesis induced by ionizing radiation through inducing apoptosis in neurogenic zones and activating microglia [19]. These novel findings may provide a new therapeutic way to prevent and inhibit the radiation-induced pathogenesis of depression. In this study, we found that low dose rate irradiation induced up-regulation of miR-448-3p and miR-361-5p, but down-regulation of miR-193a-3p. miR-448-3p has been poorly studied so far. Very limited literature indicated its role in the development of cerebral aneurysms [33,34] and cerebral ischemic injury [35] through the interaction with its direct target Kruppel-like transcription factor 5 (Klf5) or nuclear factor erythroid 2-related factor 2 (Nrf2). In the former [33], miR-448-3p showed an anti-inflammatory effect by reducing Klf5, MMP2 and MMP5, which may prevent the low dose rate irradiation-induced glial activation. Whereas in the latter [34], upregulation of miR-448-3p was observed after brain injury. Meanwhile, the observation that down-regulation of miR-448-3p reduced oxidative stress and apoptosis suggested its involvement in chronic low-dose rate radiation-induced persistent DNA damage or r-H2AX foci in the stratum granulosum of the dentate gyrus as failure to repair DNA damage may lead to apoptosis.

miR-361-5p was proven to promote oxygen-glucose deprivation/re-oxygenation-induced neuronal injury in vitro by regulating sequestosome 1 (SQSTM1) [36]. It was associated with PARP1, ubiquitin-protein ligase E3 component N-recognin 5 (UBR5) and ataxia-telangiectasia mutated interactor (ATMIN) in tumours, which are enriched in DNA damage and repair [37–39]. miR-361-5p upregulation could reduce UBR5 expression [38], therefore inhibit ATMIN ubiquitination, attenuate the restoration of ATM and impair DNA repair [39]. The evidence that overexpression of miR-361-5p enhanced apoptosis and Bax expression, but reduced Bcl-2 [38], and miR-361-5p mimics evidently impaired the DNA repair and cell viability in UV-irradiated 661W cells [40], suggesting its involvement in low dose rate irradiation-induced DNA damage. miR-193a-3p induced the accumulation of intracellular reactive oxygen species (ROS) and DNA damage as determined by the level of γH2AX in the glioma cell line by targeting myeloid cell leukaemia 1 (Mcl-1) [41]. The down-regulation of miR-193a-3p decreased the chemoresistance and radioresistance of oesophageal squamous cell carcinoma (ESCC) cells via the presenilin 1 (PSEN1) gene [42]. In the present study, down-regulation of miR-193a-3p may reduce the accumulation of intracellular ROS, and antagonize miR-448-3p and miR-361-5p up-regulation-induced DNA damage to produce a beneficial effect.

Combined mRNA sequencing and qRT-PCR results showed the decreased expression of Ccn1, Fli1, Fosb, Ets1, Hs3st5, and Eif4ebp1, and the up-regulation of Cort, Foxh1, and Opalin in the hippocampus. Database searching by miRDB and TargetScan predicted that FLI1 and HS3ST5 are the targets of miR-448-3p. Eif4ebp2 is the target of miR-361-5p. Fli-1, as a member of the ETS transcription factor family, was first identified in Friend Murine Leukemia Virus induced erythroleukemias in 1990 by Ben-David et al.[43]. Fli1 exerts its functions in the development of hematopoietic stem cells, angiogenesis, and vasculogenesis [44]. Abnormal expression of FLI1 induced different kinds of human cancers and auto-immune diseases [45,46]. FLI1 has been broadly studied in Ewing's sarcoma, but its function in gamma radiation-induced injury has barely touched. FLI1 was found to regulate the radiotherapy resistance in nasopharyngeal carcinoma through PI3K/AKT signalling pathway [47]. Overexpression of FLI1 in glioblastoma cells promoted resistance to radiation exposure [48]. Moreover, other members of the ETS family, e.g., ERG and ETS2, were also related to the repair of DNA damage [49]. Our results showed the down-regulated expression of FlI1 in mice exposed to chronic post-natal low-dose-rate radiation, demonstrating that FLI1 as a radio sensitivity regulator may serve as a DNA damage marker in radiation research. HS3ST5 is one of seven heparan sulfate 3-O-sulfotransferase enzymes [50]. It is related with dementia and amyotrophic lateral sclerosis [51]. The aberrations of Hs3st5 gene were associated with intellectual disability and microcephaly with pontine and cerebellar hypoplasia [52]. However, no information is available regarding the role of

 doi:10.20944/preprints202408.2168.v1

Hs3st5 in DNA damage or radiation research. Our study is the first to detect the decreased expression of Hs3st5 in mice after gamma radiation exposure. Moreover, both FLI1 and Hs3st5 are the predicted targets of miR-448-3p. The interaction of miR-448-3p with both FLI1 and HS3ST5 might play a crucial role in gamma radiation-induced DNA damage in mice. Eif4ebp2 is a member of the eukaryotic translation initiation factor 4E binding protein family. The products of this family bind eIF4E and act as negative regulators of mRNA translation. Eif4ebp2 is highly expressed in the brain and regulates neuronal stem cell renewal and synapse activity through repressing translation initiation [53]. Gene expression analysis showed that the expression level of Eif4ebp2 was higher in the radiosensitive breast cancer cells when compared to the radioresistant cells [54], suggesting that Eif4ebp2 might be a biomarker of radiotherapy reaction in breast cancer. However, its function in radiation-induced DNA damage in normal animals has not been studied. The down-regulated Eif4ebp2 probably serves as a biomarker for gamma radiation-induced injury too. Nevertheless, more studies are still needed to confirm the exact role of Eif4ebp2 in gamma radiation exposure and its underlying mechanisms.

4.6. Chronic Low Dose Rate Irradiation Induced miRNA and mRNA Changes in the Blood

miRNA and mRNA sequencing of whole blood indicated a total of 186 and 462 differentially expressed miRNAs and mRNAs between the control and experimental groups respectively. Among those miRNAs and mRNAs validated by qRT-PCR, further bioinformatic analysis revealed a predicted interaction of miR-6967-3p and S1pr5. Sphingosine 1-phosphate (S1P) and its five-specific high-affinity receptor (S1PR) subtypes S1PR1–5, have significant regulatory effects in normal physiology, brain and cardiac development, inflammation, angiogenesis, vascular permeability, and cancer growth and metastasis [55]. S1PR1 was the first of this family to be discovered in 1990 [56], and is one of the most widely studied receptors of S1P. S1PR1 and S1PR5 are expressed by several cell types of the central nervous system including microglia which produce pro-inflammatory cytokines and molecules [57], and are closely related to Parkinson's disease [58]. S1PR1 and 5 were transiently induced in C57BL6/J mice after transient middle cerebral artery occlusion for 30 min [59]. However, as S1PR5 has not been extensively studied and miR-6967-3p is a relatively new miRNA, the role of their interaction in gamma irradiation-induced injury has not been clarified.

Venn analysis between blood and hippocampus indicated that 18 miRNAs and 2 mRNAs are differentially expressed. Among them, 5 down-regulated miRNAs, 2 up-regulated miRNA, and 2 down-regulated mRNAs were expressed in the same pattern in both hippocampus and blood. The results indicated that irradiation-induced blood miRNA or mRNA changes may reflect the changes of corresponding genes in the hippocampus. In other words, blood biomarker testing may provide information on the gamma irradiation-induced damage to body organs.

In summary, this study systemically examined the effects of chronic post-natal low-dose-rate gamma irradiation on the neurobehaviour, hippocampal cellular and molecular biological changes in female mice. Compared to our previous study of acute high-dose rate radiation exposure to P3 mice [12,17–19,60], chronic low-dose rate irradiation with the same cumulative dose of 5Gy significantly diminish the neuropathological changes and subsequent neurocognitive and neuropsychiatric changes. Although this chronic gamma irradiation did not induce any significant changes in the body weight, animal neurobehaviours, hippocampal cellularity, the DNA damage indicated by r-H2AX immunostaining was observed at 16 months post-irradiation. This non-recoverable DNA damage might be related to the interactions between miR-448-3p with FLI1 and/or HS3ST5, or miR-361-5p with EIF4EBP2 in the hippocampus. The functional significance of the interaction between miR-6967-3p and S1PR5 in blood remains to be investigated.

Author Contributions: Conceptualization, F.R.T., methodology, F.R.T., H.W., investigation, H.W., S.L., A.T. data curation, F.R.T.; H.W., writing: original draft preparation, H.W.; writing review and editing, F.R.T., supervision, F.R.T.; funding acquisition, F.R.T., All authors have read and agreed to the published version of the manuscript.

Funding: This research was funded by the National Research Foundation of Singapore.

Institutional Review Board Statement: All experiments were conducted according to the Institutional Animal Care and Use Committee (IACUC), National University of Singapore (IACUC number: R20-0220).

 doi:10.20944/preprints202408.2168.v1

Informed Consent Statement: Not applicable.

Data Availability Statement: The data presented in this study are available on request from the corresponding author.

Acknowledgments: This study was supported by grants from the National Research Foundation of Singapore to the Singapore Nuclear Research and Safety Initiative (F.R.T.). The technical support from Kael Lee Koon Lam is greatly appreciated.

Conflicts of Interest: The authors declare no conflict of interest.

References

1. Kimler, B., *Prenatal irradiation: a major concern for the developing brain.* International Journal of Radiation Biology, 1998. **73**(4): p. 423-434.
2. Setkowicz, Z. and K. Janeczko, *A strong epileptogenic effect of mechanical injury can be reduced in the dysplastic rat brain: Long-term consequences of early prenatal gamma-irradiation.* Epilepsy research, 2005. **66**(1-3): p. 165-172.
3. Setkowicz, Z., et al., *Brain dysplasia evoked by gamma irradiation at different stages of prenatal development leads to different tonic and clonic seizure reactivity.* Epilepsy research, 2014. **108**(1): p. 66-80.
4. Nakahira, R., et al., *Effects of Continuous* In Utero *Low- and Medium-Dose-Rate Gamma-Ray Exposure on Fetal Germ Cells.* Radiat Res, 2021. **195**(3): p. 235-243.
5. Tang, F., et al., *Effects of Continuous Prenatal Low Dose Rate Irradiation on Neurobehavior, Hippocampal Cellularity, mRNA and miRNA Expression on B6C3F1 Mice*, in *Preprints*. 2024, Preprints.
6. Otake, M., *Threshold for radiation-related severe mental retardation in prenatally exposed A-bomb survivors: a re-analysis.* International journal of radiation biology, 1996. **70**(6): p. 755-763.
7. Otake, M. and W.J. Schull, In utero *exposure to A-bomb radiation and mental retardation; a reassessment.* The British journal of radiology, 1984. **57**(677): p. 409-414.
8. Fushiki, S., *Radiation hazards in children–lessons from Chernobyl, Three Mile Island and Fukushima.* Brain and Development, 2013. **35**(3): p. 220-227.
9. Palgi, Y., et al., *Mental health and disaster related attitudes among Japanese after the 2011 Fukushima nuclear disaster.* 2012.
10. Stepanova, E.I., A. Misharina Zh, and V. Vdovenko, *[Long-term cytogenetic effects in children prenatally-exposed to radiation as a result of the accident at the Chernobyl Atomic Energy Station].* Radiats Biol Radioecol, 2002. **42**(6): p. 700-3.
11. Geets, W., *Possible influence of pre-natal irradiation on the development of cerebral electrical activity in man.* Electroencephalogr Clin Neurophysiol, 1968. **25**(4): p. 417.
12. Wang, H., et al., *Early Life Irradiation-Induced Hypoplasia and Impairment of Neurogenesis in the Dentate Gyrus and Adult Depression Are Mediated by MicroRNA- 34a-5p/T-Cell Intracytoplasmic Antigen-1 Pathway.* Cells, 2021. **10**(9).
13. Atamanyuk, N.I., et al., *The Dose-Dependent Effect of Fractionated γ-Radiation on Anxiety-Like Behavior in Neonatal Mice.* Bull Exp Biol Med, 2024. **176**(6): p. 727-730.
14. Tanaka, S., et al., *No lengthening of life span in mice continuously exposed to gamma rays at very low dose rates.* Radiat Res, 2003. **160**(3): p. 376-9.
15. Tanaka, I.B., 3rd, et al., *Cause of death and neoplasia in mice continuously exposed to very low dose rates of gamma rays.* Radiat Res, 2007. **167**(4): p. 417-37.
16. Liu, Y., et al., *Neonatal exposure to low-dose X-ray causes behavioral defects and abnormal hippocampal development in mice.* IUBMB Life, 2023. **75**(6): p. 530-547.
17. Tang, F.R., et al., *Spatiotemporal dynamics of γH2AX in the mouse brain after acute irradiation at different postnatal days with special reference to the dentate gyrus of the hippocampus.* Aging (Albany NY), 2021. **13**(12): p. 15815-15832.
18. Ren, B.X., et al., *Early postnatal irradiation-induced age-dependent changes in adult mouse brain: MRI based characterization.* BMC Neurosci, 2021. **22**(1): p. 28.
19. Wang, H., et al., *Dual Effects of miR-181b-2-3p/SOX21 Interaction on Microglia and Neural Stem Cells after Gamma Irradiation.* Cells, 2023. **12**(4).
20. Nakada, T., et al., *The Effects of Low-Dose-Rate γ-irradiation on Forced Swim Test-Induced Immobility and Oxidative Stress in Mice.* Acta Med Okayama, 2021. **75**(2): p. 169-175.
21. Ma, T., et al., *Low-dose-rate induces more severe cognitive impairment than high-dose-rate in rats exposed to chronic low-dose γ-radiation.* Front Public Health, 2024. **12**: p. 1387330.
22. Schmitz, C., et al., *Prenatal protracted irradiation at very low dose rate induces severe neuronal loss in rat hippocampus and cerebellum.* Neuroscience, 2005. **130**(4): p. 935-48.
23. Rothkamm, K. and S. Horn, *gamma-H2AX as protein biomarker for radiation exposure.* Ann Ist Super Sanita, 2009. **45**(3): p. 265-71.

24. Ramadhani, D., et al., *γ-H2AX and phospho-ATM enzyme-linked immunosorbent assays as biodosimetry methods for radiation exposure assessment: a pilot study.* Radiat Prot Dosimetry, 2023. **199**(19): p. 2383-2390.
25. Podhorecka, M., A. Skladanowski, and P. Bozko, *H2AX Phosphorylation: Its Role in DNA Damage Response and Cancer Therapy.* J Nucleic Acids, 2010. **2010**.
26. Raavi, V., V. Perumal, and F.D.P. S, *Potential application of γ-H2AX as a biodosimetry tool for radiation triage.* Mutat Res Rev Mutat Res, 2021. **787**: p. 108350.
27. Chen, Z., et al., *Radiation exposure lymphocyte damage assessed by γ-H2AX level using flow cytometry.* Sci Rep, 2024. **14**(1): p. 4339.
28. Zhao, H., et al., *An estimate assay for low-level exposure to ionizing radiation based on mass spectrometry quantification of γ-H2AX in human peripheral blood lymphocytes.* Front Public Health, 2022. **10**: p. 1031743.
29. Moroni, M., et al., *Evaluation of the gamma-H2AX assay for radiation biodosimetry in a swine model.* Int J Mol Sci, 2013. **14**(7): p. 14119-35.
30. Fardid, R., et al., *Evaluation of the relationship between γ-H2AX biomarker levels and dose received after radiation exposure in abdominal-pelvic and chest CT scans.* J Cancer Res Ther, 2023. **19**(5): p. 1392-1397.
31. Redon, C.E., et al., *The use of gamma-H2AX as a biodosimeter for total-body radiation exposure in non-human primates.* PLoS One, 2010. **5**(11): p. e15544.
32. Segaran, R.C., et al., *Neuronal Development-Related miRNAs as Biomarkers for Alzheimer's Disease, Depression, Schizophrenia and Ionizing Radiation Exposure.* Curr Med Chem, 2021. **28**(1): p. 19-52.
33. Zhang, J.Z., et al., *miR-448-3p controls intracranial aneurysm by regulating KLF5 expression.* Biochem Biophys Res Commun, 2018. **505**(4): p. 1211-1215.
34. Boga, Z., et al., *The Role of miR-26a, miR-29a and miR-448-3p in the Development of Cerebral Aneurysm.* Turk Neurosurg, 2023. **33**(3): p. 423-430.
35. Xu, M., et al., *Inhibition of miR-448-3p Attenuates Cerebral Ischemic Injury by Upregulating Nuclear Factor Erythroid 2-Related Factor 2 (Nrf2).* Neuropsychiatr Dis Treat, 2021. **17**: p. 3147-3158.
36. Zeng, T., et al., *MiR-361-5p promotes oxygen-glucose deprivation/re-oxygenation induced neuronal injury by negatively regulating SQSTM1 in vitro.* Metab Brain Dis, 2021. **36**(8): p. 2359-2368.
37. Tommasi, S., et al., *miR-151-5p, targeting chromatin remodeler SMARCA5, as a marker for the BRCAness phenotype.* Oncotarget, 2016. **7**(49): p. 80363-80372.
38. Jia, J., et al., *MicroRNA-361-5p slows down gliomas development through regulating UBR5 to elevate ATMIN protein expression.* Cell Death Dis, 2021. **12**(8): p. 746.
39. Li, C.G., et al., *PPARγ Interaction with UBR5/ATMIN Promotes DNA Repair to Maintain Endothelial Homeostasis.* Cell Rep, 2019. **26**(5): p. 1333-1343.e7.
40. Huang, Y., et al., *Transcriptome Sequencing Reveals Tgf-β-Mediated Noncoding RNA Regulatory Mechanisms Involved in DNA Damage in the 661W Photoreceptor Cell Line.* Genes (Basel), 2022. **13**(11).
41. Kwon, J.E., et al., *Ionizing radiation-inducible microRNA miR-193a-3p induces apoptosis by directly targeting Mcl-1.* Apoptosis, 2013. **18**(7): p. 896-909.
42. Meng, F., et al., *miR-193a-3p regulation of chemoradiation resistance in oesophageal cancer cells* via *the PSEN1 gene.* Gene, 2016. **579**(2): p. 139-45.
43. Ben-David, Y., E.B. Giddens, and A. Bernstein, *Identification and mapping of a common proviral integration site Fli-1 in erythroleukemia cells induced by Friend murine leukemia virus.* Proc Natl Acad Sci U S A, 1990. **87**(4): p. 1332-6.
44. Bonetti, P., et al., *Deregulation of ETS1 and FLI1 contributes to the pathogenesis of diffuse large B-cell lymphoma.* Blood, 2013. **122**(13): p. 2233-41.
45. Li, Y., et al., *The ets transcription factor Fli-1 in development, cancer and disease.* Oncogene, 2015. **34**(16): p. 2022-31.
46. Ma, Y., et al., *Fli-1 Activation through Targeted Promoter Activity Regulation Using a Novel 3′, 5′-diprenylated Chalcone Inhibits Growth and Metastasis of Prostate Cancer Cells.* Int J Mol Sci, 2020. **21**(6).
47. Chen, E., et al., *FLI1 regulates radiotherapy resistance in nasopharyngeal carcinoma through TIE1-mediated PI3K/AKT signaling pathway.* J Transl Med, 2023. **21**(1): p. 134.
48. Rajesh, Y., et al., *Transcriptional regulation of HSPB1 by Friend leukemia integration-1 factor modulates radiation and temozolomide resistance in glioblastoma.* Oncotarget, 2020. **11**(13): p. 1097-1108.
49. Sizemore, G.M., et al., *The ETS family of oncogenic transcription factors in solid tumours.* Nat Rev Cancer, 2017. **17**(6): p. 337-351.
50. Ota, H. and S. Nishihara, *Regulation of 3-O-Sulfation of Heparan Sulfate During Transition from the Naïve to the Primed State in Mouse Embryonic Stem Cells.* Methods Mol Biol, 2022. **2303**: p. 443-452.
51. Wainberg, M., S.J. Andrews, and S.J. Tripathy, *Shared genetic risk loci between Alzheimer's disease and related dementias, Parkinson's disease, and amyotrophic lateral sclerosis.* Alzheimers Res Ther, 2023. **15**(1): p. 113.
52. Hayashi, S., et al., *Comprehensive investigation of CASK mutations and other genetic etiologies in 41 patients with intellectual disability and microcephaly with pontine and cerebellar hypoplasia (MICPCH).* PLoS One, 2017. **12**(8): p. e0181791.

 doi:10.20944/preprints202408.2168.v1

53. Bidinosti, M., et al., *Postnatal deamidation of 4E-BP2 in brain enhances its association with raptor and alters kinetics of excitatory synaptic transmission.* Mol Cell, 2010. **37**(6): p. 797-808.
54. Meehan, J., et al., *A Novel Approach for the Discovery of Biomarkers of Radiotherapy Response in Breast Cancer.* J Pers Med, 2021. **11**(8).
55. Bryan, A.M. and M. Del Poeta, *Sphingosine-1-phosphate receptors and innate immunity.* Cell Microbiol, 2018. **20**(5): p. e12836.
56. Hla, T. and T. Maciag, *An abundant transcript induced in differentiating human endothelial cells encodes a polypeptide with structural similarities to G-protein-coupled receptors.* J Biol Chem, 1990. **265**(16): p. 9308-13.
57. Gruchot, J., et al., *Siponimod Modulates the Reaction of Microglial Cells to Pro-Inflammatory Stimulation.* Int J Mol Sci, 2022. **23**(21).
58. Chen, X., et al., *Integrative analysis of potential biomarkers and immune cell infiltration in Parkinson's disease.* Brain Res Bull, 2021. **177**: p. 53-63.
59. Matsumoto, N., et al., *Up-regulation of sphingosine-1-phosphate receptors and sphingosine kinase 1 in the peri-ischemic area after transient middle cerebral artery occlusion in mice.* Brain Res, 2020. **1739**: p. 146831.
60. Liu, L., et al., *Radiosensitivity-related Variation in MicroRNA-34a-5p Levels and Subsequent Neuronal Loss in the Hilus of the Dentate Gyrus after Irradiation at Postnatal Days 10 and 21 in Mice.* Radiat Res, 2024.